Effect of austenitizing temperature and cooling rate on the structure and properties of a ultrahigh strength low alloy steel

N. KISHORE BABU
Department of Metallurgical Engineering, Banaras Hindu University, Varanasi 220015, India
E-mail: kishore_pandu@yahoo.com

M. R. SURESH*, P. P. SINHA
Vikram Sarabhai Space Centre, ISRO, Trivandrum 695022, India
E-mail: mrsuresh61@rediffmail.com; pp_sinha@vssc.org

D. S. SARMA
Department of Metallurgical Engineering, Banaras Hindu University, Varanasi 220015, India
E-mail: dssarma1@rediffmail.com

Published online: 28 March 2006

A 0.3C-CrMoV(ESR) steel is being developed primarily for making pressure vessels used for aerospace applications. Since it is important to understand the range of microstructures and mechanical properties that will be obtained in the heat affected zone of welds, the steel has been subjected to different austenitizing treatments (temperatures ranging from 925°C to 1250°C) followed by cooling at various rates to room temperature. It has been shown that the austenite grain size increased from about 10 to 250 μm as the austenitizing temperature is increased from 925°C to 1250°C (1 hr) and that the hardness, YS, UTS,% elongation and% reduction in area as well as CVN energy for 450°C tempered condition decrease as the austenitizing temperature is increased for all cooling rates (furnace cooling, air cooling, oil quenching, quenching and tempering at 450°C). This is attributed mainly to the increase in austenitic grain size. The ranges of microstructures that can be obtained in the heat-affected zone are massive ferrite, fine pearlite, upper as well as lower bainite and martensite. The Charpy impact energy for the oil-quenched steel tempered at 200°C, however, did not vary significantly with austenitizing temperature.

1. Introduction

The materials used for air-borne structures should have high specific strength, high fracture toughness, and ease of fabrication and heat treatment. Low alloy steels like AFNOR 15CDV6 [1, 2], D6AC [3], etc. have been used as materials for solid propellant rocket motor casings. A low alloy steel with a nominal composition of 0.3%C-1.5%Cr-1%Mo-0.2%V-0.1%Nb, designated 0.3C-CrMoV(ESR), is being developed for similar applications and it has been shown that it has high specific strength and good toughness when quenched and tempered [4–6]. In order to get extra-low levels of sulphur and oxides, the Electro-Slag Remelting (ESR) method [7] was used for secondary refining. ESR is an effective remelting process in eliminating oxide and sulphide inclusions in steels. In this, the steel to be refined is made in the form of a cast or rolled bar and is progressively melted by immersing its lower end in a resistance heated bath of molten superheated slag held in a water-cooled copper or mild steel mould. Steel processed through ESR possesses improved cleanliness, fatigue resistance, fracture and notch toughness, ductility, weldability, corrosion resistance and isotropy in properties.

Since different regions of heat affected zone of a weld experience a wide range of temperatures in the austenite field and also subjected to varied cooling rates, the present work has been taken up to study the influence of

*Author to whom all correspondence should be addressed.
0022-2461
DOI: 10.1007/s10853-006-6718-1

TABLE I. Chemical composition (in wt%) of the steel used in the present investigation

Alloying element	wt.%
Carbon	0.29
Manganese	0.90
Sulphur, max	0.015
Phosphorous, max	0.02
Chromium	1.40
Molybdenum	0.90
Vanadium	0.25
Niobium	0.10
Silicon	0.25

austenitizing temperature and cooling rate on the structure and properties of the present steel. For this purpose, the steel has been heated to varying temperatures in the range 925–1250°C followed by cooling in furnace, air and oil and the influence of these treatments on the structure and properties has been evaluated.

2. Experimental procedures

The steel was primarily melted in an electric arc furnace followed by sand-casting into a cylindrical ingot that was then used as the consumable electrode in an electroslag refining furnace for secondary refining. The melt was inoculated using niobium during ESR to refine the grain structure. The steel was produced as ESR-cast ingot of 600 mm diameter. The chemical composition of the steel is given in Table I.

The cast ingot was subsequently hot rolled to plates of 8 mm thickness. Tensile blanks of $75 \times 16 \times 8$ mm size and Charpy impact specimen blanks of size $55 \times 11 \times 8$ mm cut from the hot rolled plates were austenitized for 1 hour at different temperatures of 925°C, 1000°C, 1100°C, 1200°C or 1250°C. The upper critical point for this steel has been observed to be in the vicinity of 865°C. They were then subjected to furnace cooling, air-cooling or oil quenching to room temperature. The cooling rates for furnace cooling, air cooling and oil quenching are 0.10°C/s, 10°C/s and 500°C/s respectively. The oil-quenched blanks were tempered at two different tempering temperatures viz. 200°C or 450°C for 2 hours in each case. After heat treatment, the blanks were machined to final dimensions.

Vickers hardness tests were carried out using 10 kg load on polished specimens. An average of three readings was reported as the bulk hardness of the material.

Cylindrical (shouldered) tensile specimens of 16 mm gauge length and 4.5 mm diameter were machined from heat-treated blanks. Tensile testing was carried out in an INSTRON universal testing machine using a load cell of 5000 kg. and a cross-head speed of 0.50 mm/minute with a strain rate of approximately 0.1/min. The tensile properties based on two tensile tests for each condition are reported.

Sub-size Charpy specimens of $55 \times 10 \times 5$ mm size with a V-notch were machined from the heat treated Charpy blanks and tested at ambient temperature.

Optical microscopic studies were made on conventionally prepared specimens etched with 2% nital solution. For transmission electron microscopy, thin slices of thickness 0.125 mm were cut from the specimens on a Buehler Isomet low speed saw and they were further thinned by mechanical polishing to 0.03 mm. Discs of 3 mm diameter, punched off from these slices, were electro-polished using 90% acetic acid solution at 30–35 V, at 10°C. The thin foils were examined in a JEOL CX-200 Transmission Electron Microscope operating at 160 kV.

3. Results

3.1. Mechanical properties

The variation in hardness with austenitizing temperature for various conditions of heat treatment is shown in Fig. 1. It is seen that the hardness decreased gradually as the austenitizing temperature is increased from 925°C to 1250°C; from 598 to 516 VHN for oil quenched condition and from 420 to 323 VHN in the case of furnace-cooled samples.

Fig. 2 shows the influence of austenitizing temperature on yield strength (YS) for different conditions of heat treatment studied. Among all austenitizing temperatures studied, the yield strength has been observed to be the maximum for samples austenitized at 925°C for all cooling conditions employed, and then it decreased as the austenitizing temperature was increased to 1250°C. For the oil quenched samples, the YS decreased from 1427 MPa to 1187 MPa while the decrease was from 1029 MPa to 839 MPa in furnace cooled samples. The YS for specimens tempered at 200°C after austenitizing at different temperatures ranging from 925°C to 1250°C varied from 1437 MPa to 1088 MPa, while the corresponding values are 1395 MPa and 989 MPa for the steel tempered at 450° C.

The influence of austenitizing temperature on ultimate tensile strength (UTS) for different heat treatment conditions is shown in Fig. 3. The maximum value of UTS occurred for the steel when austenitized at 925°C for all cooling conditions under study. It gradually decreased from 1762 MPa to 1489 MPa for oil-quenched samples as the austenitizing temperature was increased from 925°C to 1250°C. For furnace-cooled samples, the corresponding values ranged from 1174 MPa to 1009 MPa. Tempering at 200°C after oil quenching decreased the UTS from 1725 MPa to 1411 MPa, while tempering at 450°C resulted in a decrease from 1510 MPa to 1283 MPa.

The variation in percentage elongation with austenitizing temperature for different heat treatment conditions is shown in Fig. 4. The elongation decreased from 16% to 11% for samples in furnace-cooled condition, while it varied from 12.5% to 8% for oil-quenched samples

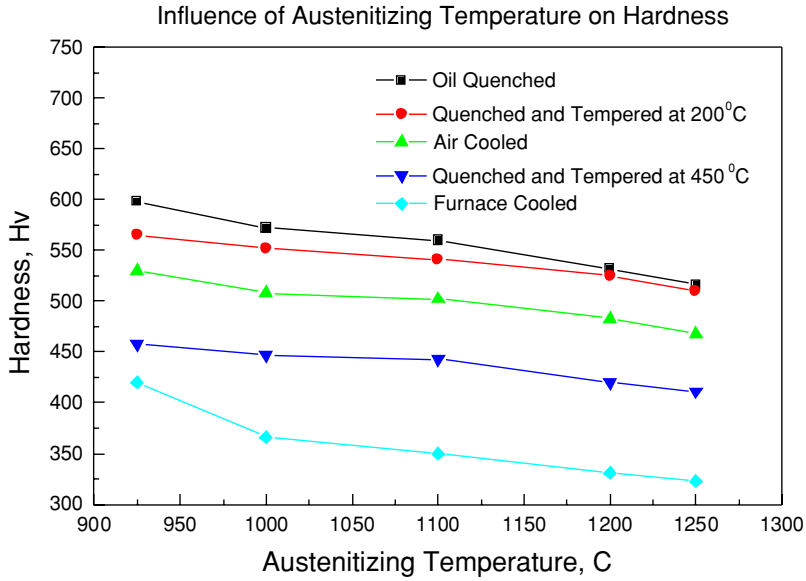

Figure 1 Variation in hardness with austenitizing temperature for various heat treatment conditions.

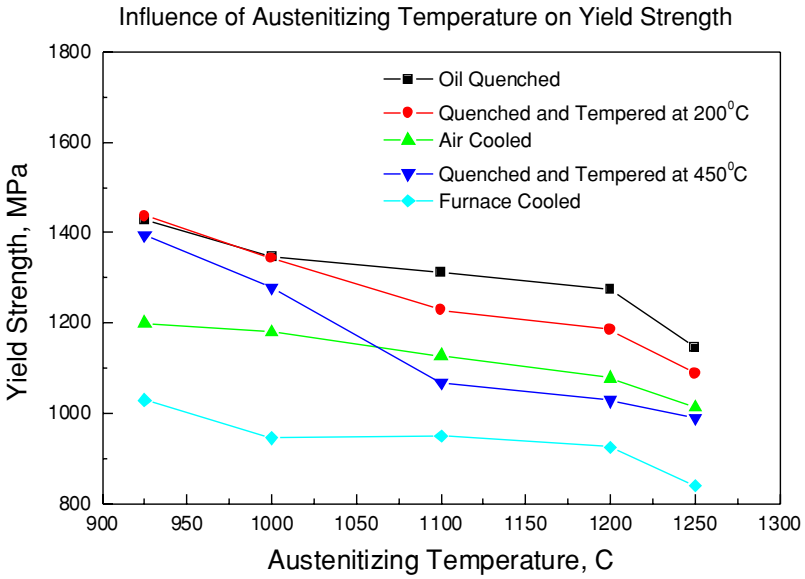

Figure 2 Influence of austenitizing temperature on yield strength for different heat treatment conditions.

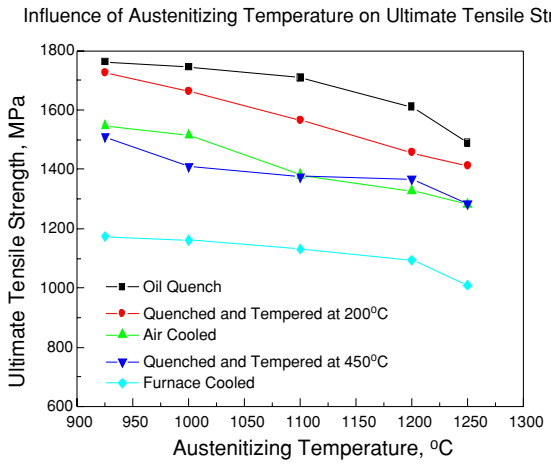

Figure 3 Influence of austenitizing temperature on ultimate tensile strength for different heat treatment conditions.

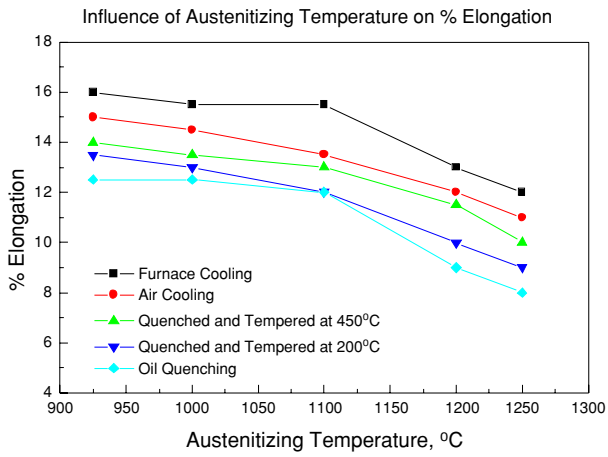

Figure 4 Variation in elongation with austenitizing temperature for different heat treatment conditions.

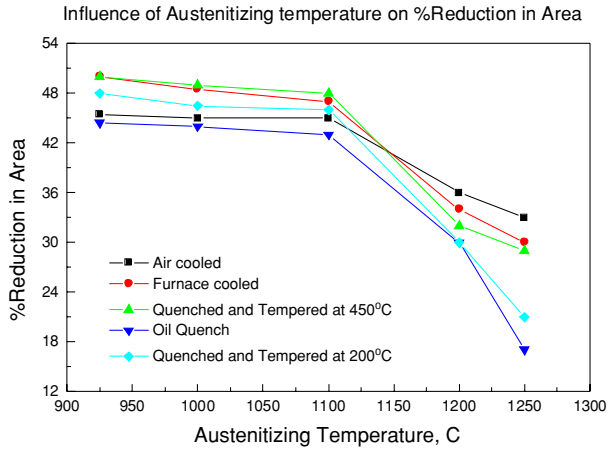

Figure 5 Variation in reduction in area with austenitizing temperature for different heat treatment conditions.

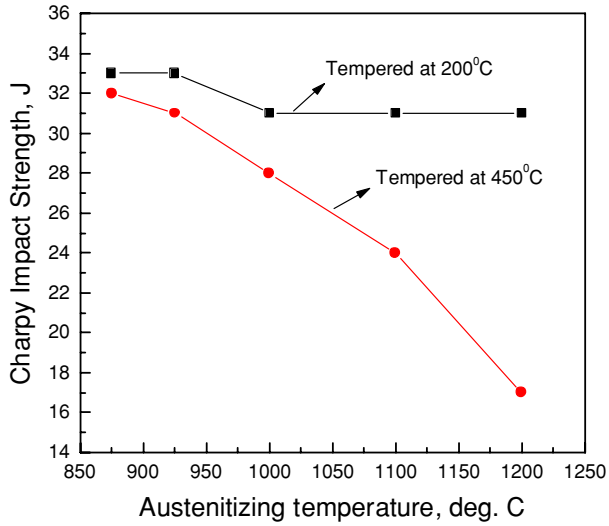

Figure 6 Variation of Charpy V-notch (CVN) energies as a function of austenitizing temperature for (OQ-200) and (OQ-450) conditions.

after austenitizing at different temperatures ranging from 925°C to 1250°C. The corresponding decrease in reduction in area, shown in Fig. 5 is from 50% to 32% for furnace-cooled samples and 45% to 17% for oil-quenched samples.

The sub-size Charpy V-notch (CVN) energies were also measured as a function of austenitizing temperature for the samples oil-quenched and tempered at 200°C (OQ-200) and 450°C (OQ-450) only and the variation is shown in Fig. 6. In all cases, the OQ-200 showed much better CVN energies compared to OQ-450 condition. For the former, the CVN decreased from 33 J to 31 J as the austenitizing temperature is increased from 925°C to 1200°C. The corresponding values for OQ-450 are 32 J and 16 J. The CVN values for the furnace-cooled and air-cooled conditions were measured only after austenitizing at 925°C and the respective values were 28 and 25 J. These values were found to be inferior to the austenitized and tempered

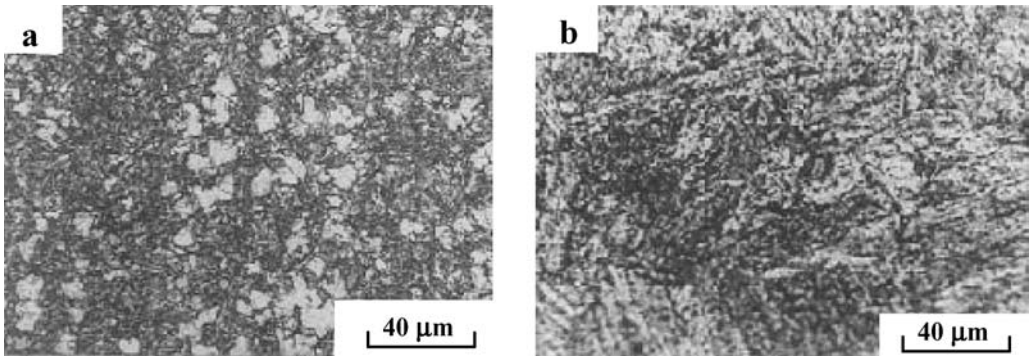

Figure 7 Optical micrograph of the steel furnace cooled (a) from 925°C showing a ferrite–pearlite structure and (b) from 1000°C showing fully bainitic structure.

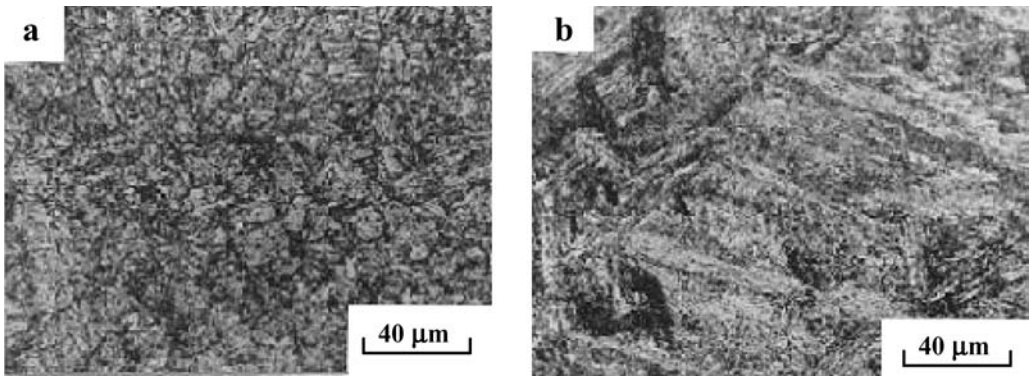

Figure 8 Optical micrograph of the steel air cooled (a) from 925°C and (b) from 1000°C showing fully bainitic structure.

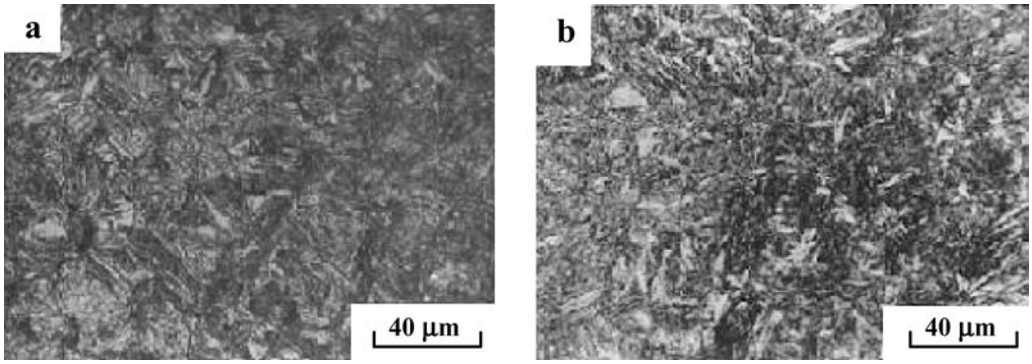

Figure 9 Typical optical micrograph of the steel oil quenched showing lath martensite structure.

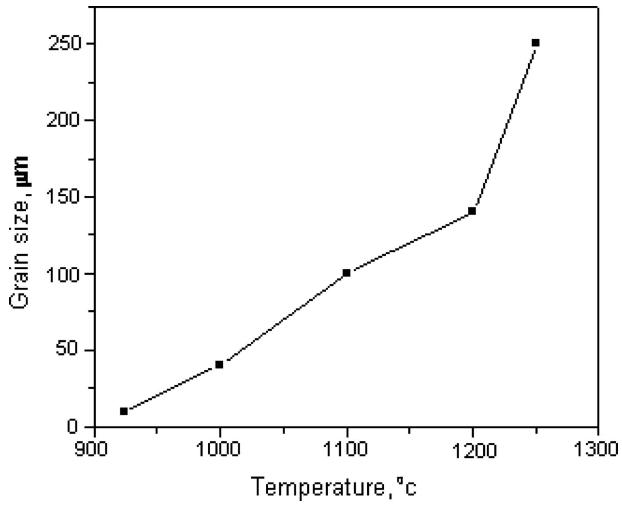

Figure 10 Variation of grain size with austenitizing temperature.

samples (OQ-200 and OQ-450) for the same austenitizing temperature.

3.2. Optical microscopy

Optical microscopy studies show that the steel when furnace-cooled from 925°C has a ferrite–pearlite structure [Fig. 7(a)] while it appears to be fully bainitic when furnace-cooled from 1000°C, as shown in Fig. 7(b). In air-cooled condition from all austenitizing temperatures, it shows complete bainitic structure as illustrated in Fig. 8(a and b). Similarly all the oil-quenched specimens irrespective of austenitizing temperatures showed lath martensite structure (Fig. 9). No noticeable change in the optical microstructure could be seen on tempering either at 200°C or 450°C.

As expected, the prior austenite grain size increased with the increasing austenitizing temperature, for example, about 10 μm at 925°C and nearly 250 μm at 1250°C (Fig. 10).

3.3. Transmission electron microscopy

Samples for transmission electron microscopy were taken from the shoulder portion of tensile specimens that were austenitized at 925°C, 1100°C and 1250°C in different quenching and tempering conditions.

Fig. 11(a–c) are the transmission electron micrographs (TEMs) of the steel furnace-cooled from 925°C, 1100°C and 1250°C showing respectively massive ferrite and extremely fine pearlite, lath ferrite having high dislocation density, and plate-like carbides at an angle to the lath boundary typical of lower bainite in low carbon steels as well as coarse carbides along the lath boundaries typical of upper bainite. Fig. 11d. gives the SAD of the cementite precipitate while Fig. 11e. is the schematic of the same.

Fig. 12(a–c) are the TEMs of the steel air-cooled from 925°C, 1100°C and 1250°C showing respectively carbides along the lath boundaries as well as within the laths typical of mixed upper and lower bainite structure (Fig. 12a and b) while at the high austenitizing temperature of 1250°C, the structure changed predominantly to upper bainite (Fig. 12c).

Fig. 13(a–c) present the TEMs of the steel oil-quenched from 925°C, 1100°C and 1250°C showing typical lath martensite structures in all conditions. Fig. 14(a and b) are the bright field and dark field transmission electron micrographs respectively of the steel oil-quenched from 925°C and tempered at 200°C showing the precipitation of fine carbides identified, in an earlier study also by selected area diffraction, as ε-carbide [4]. Similar structures were observed in the samples subjected to other austenitizing temperatures also. Fig. 14c. shows the SAD of ε-carbide precipitate and Fig. 14d. is its schematic. However, on tempering at 450°C, all the samples (austenitized at 925°C to 1250°C followed by oil quenching) showed presence of cementite platelets within the laths as well as along the lath boundaries as seen in both bright field and dark field micrographs (Fig. 15a and b) typically shown for samples austenitized at 1250°C.

4. Discussion

Suresh et al have previously demonstrated that the steel studied in the present investigation had excellent mechanical properties that were even superior to the conventional steels used for satellite launch vehicle applications [4, 5].

They attributed this to the tempered martensite structure (in the heat treated condition) of the present steel as compared to the bainite in the earlier ones. While studying the changes in microstructure and mechanical properties on tempering, they reported that the superior properties of the steel were due to the finer inclusions, finer grain size and favored texture (obtained due to the ESR process adopted). Since the preliminary studies have shown

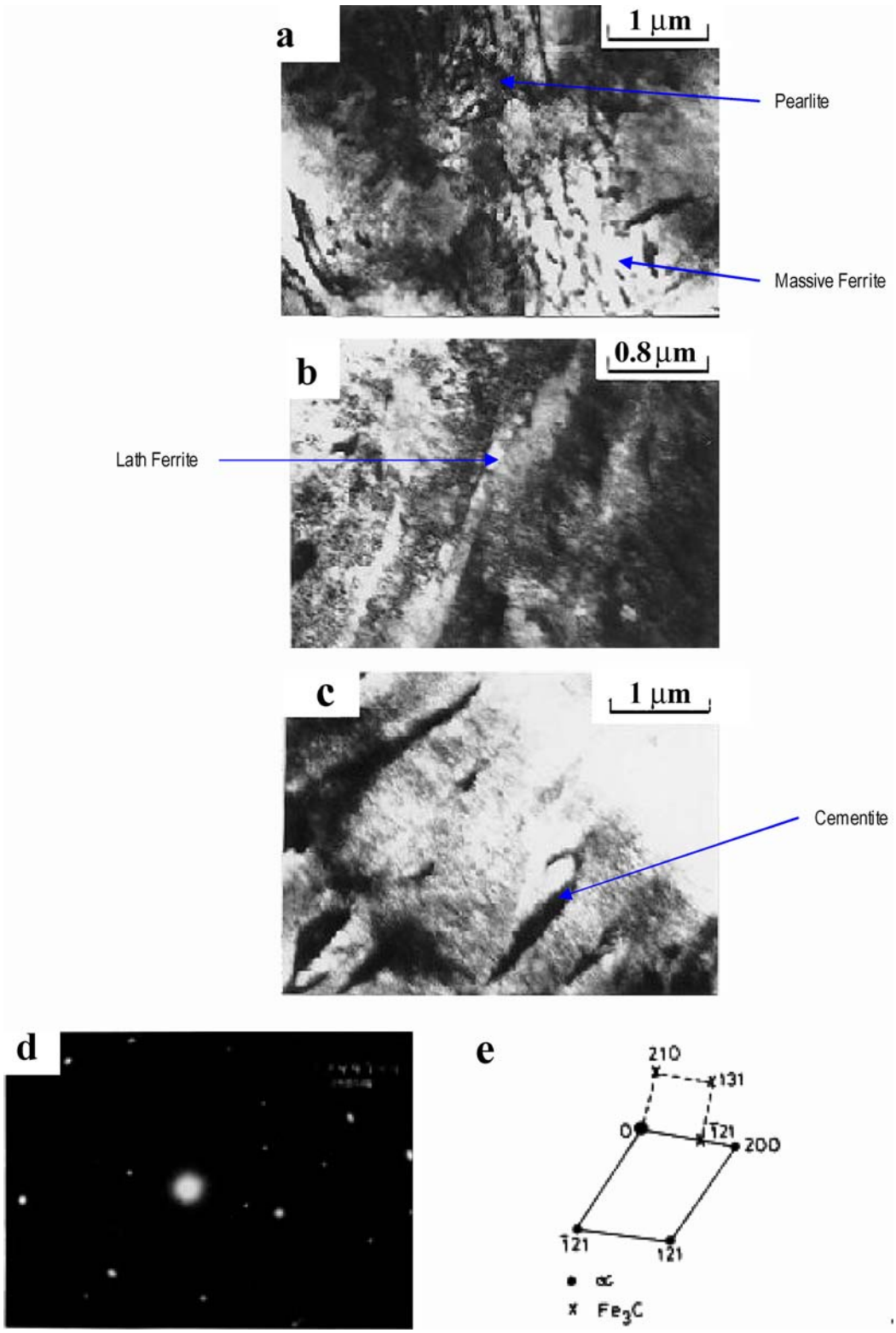

Figure 11 TEM micrographs of the steel furnace cooled (a) from 925°C showing massive ferrite and extremely fine pearlite (b) from 1100°C showing lath ferrite having high dislocation density, and (c) from 1250°C showing plate-like carbides at an angle to the lath boundary typical of lower bainite in low carbon steels as well as coarse carbide particles along the lath boundaries typical of upper bainite (d) SAD pattern (e) schematic.

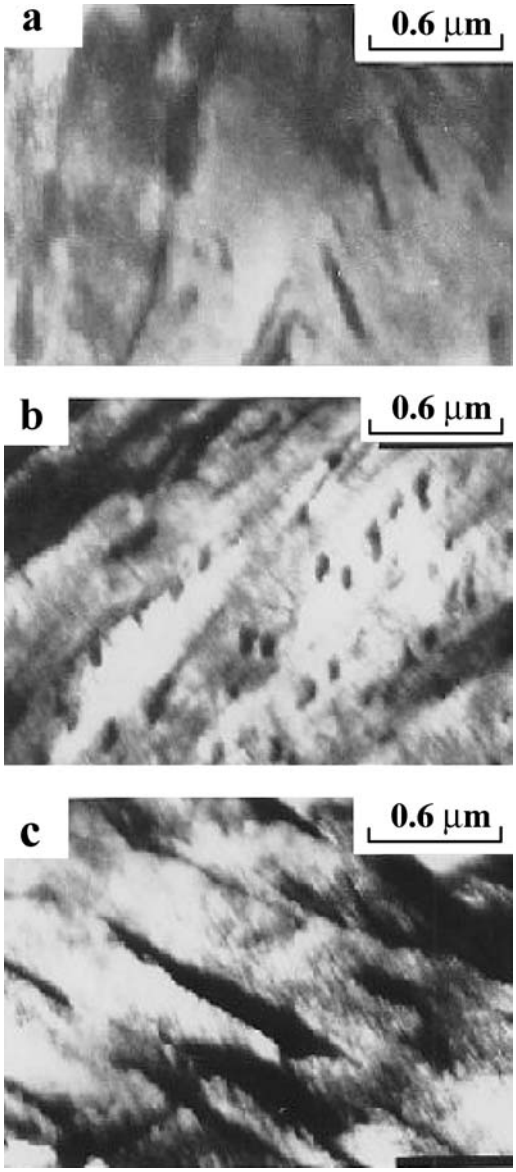

Figure 12 TEM micrographs of the steel air-cooled (a) from 925°C showing mixed upper and lower bainitic structure (b) from 1100°C showing lower bainitic structure and (c) 1250°C showing upper bainitic structure.

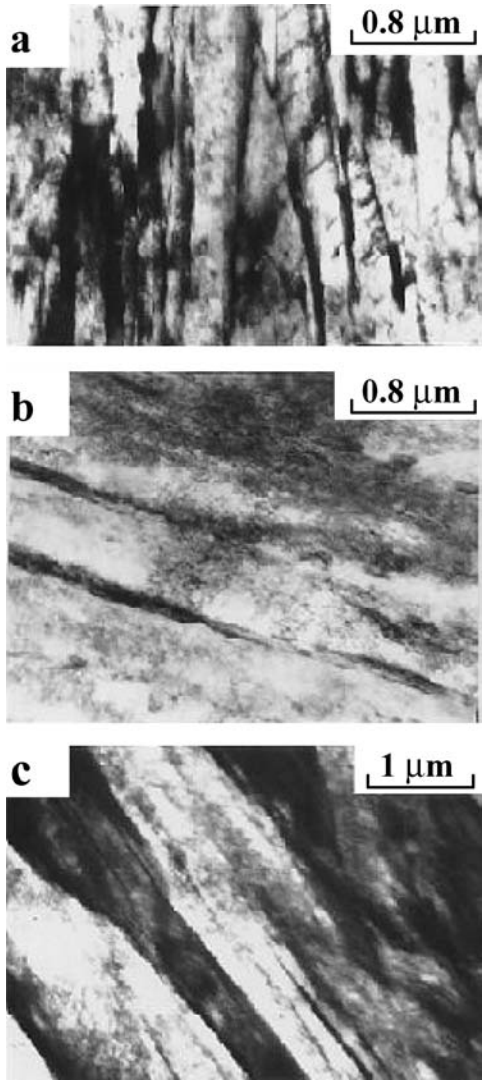

Figure 13 TEM micrographs of the steel oil-quenched from 925°C, 1100°C and 1250°C showing typical lath martensite structures in all conditions.

that the steel is satisfactorily weldable [8], the present work has been taken up to study the range of microstructures and properties obtained in the heat-affected zone in a weld.

The present investigation shows that the YS (0.2% proof strength in the present case), UTS and hardness decrease gradually with increasing austenitizing temperature in the range 925–1250°C for all the cooling rates employed, viz., furnace cooling, air cooling, oil quenching as well as for oil quenched and tempered conditions studied (Figs 1–3). The decrease was seen in the range of 9 to 12% for hardness, 18% for YS and 10–18% for UTS. For instance, the yield strength of the steel in the oil-quenched condition decreased from 1427 MPa at 925°C to 1147 MPa at 1250°C. The corresponding values for the steel tempered at 200°C were 1437 MPa and 1088 MPa respectively while for the 450°C tempering condition, they were 1395 MPa and 989 MPa respectively. Since the fall is of same percentage irrespective of widely varying initial microstructures it can be attributed mainly to the increase in grain size. There has also been a reduction in the ductility as measured by% elongation or % reduction in area with increase in austenitizing temperature (Figs 4 and 5).

Since this decrease is observed for all cooling rates, it is expected that the austenitic grain size is primarily responsible in controlling the variation in mechanical properties due to variation in austenitizing temperature. This conclusion is supported by the results of optical and transmission electron microscopy where the furnace cooled steel exhibited ferrite–pearlite structure after austenitizing at 925°C and bainitic structure at higher austenitizing temperatures; the latter microstructure should result in higher strength but it had lower strength and hardness than that austenitized at 925°C. In the case of air cooled condition or oil quenched the structures did not radically vary with austenitizing temperature and gave bainite and martensite

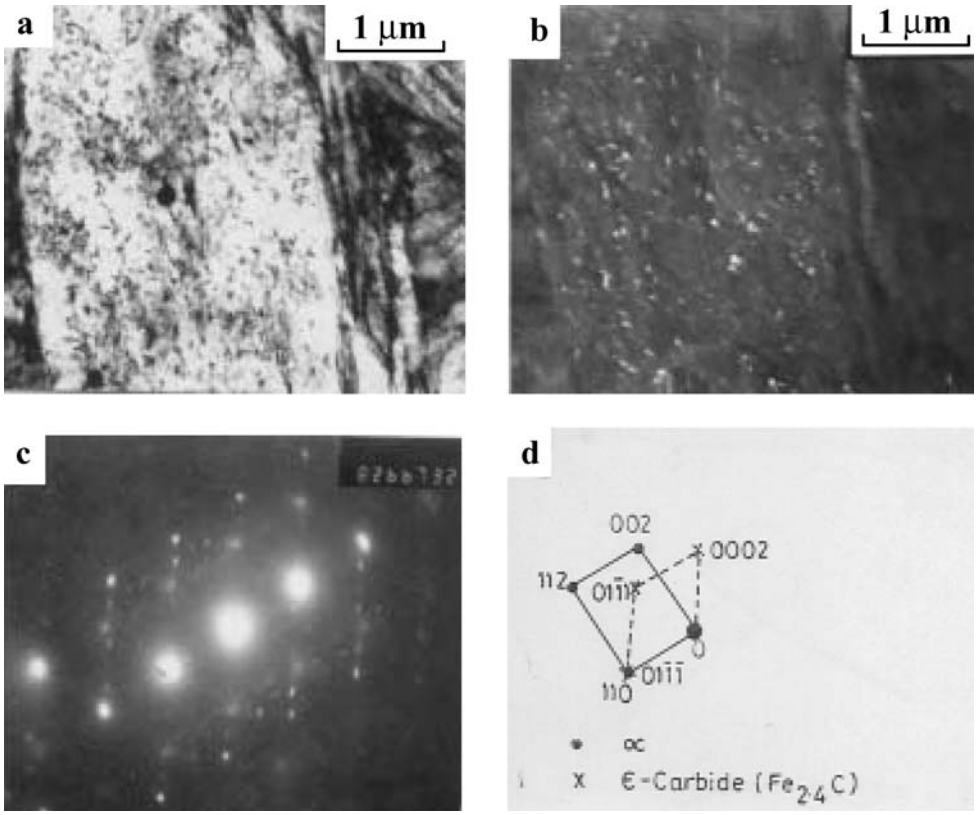

Figure 14 (a) Bright field and (b) dark field TEM micrographs of the steel oil-quenched from 925°C and tempered at 200°C showing the precipitation of fine ε-carbide (c) SAD pattern (d) schematic.

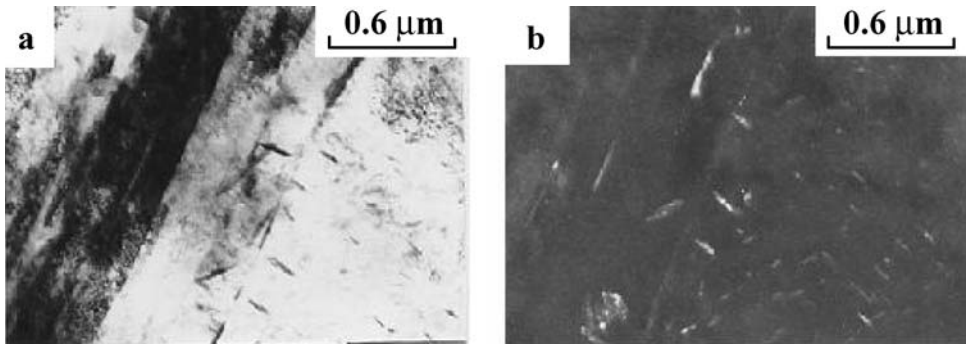

Figure 15 TEM micrographs of the steel samples austenitized at 1250°C showing cementite platelets within the lath as well as along the lath boundaries as seen in both (a) bright field and (b) dark field micrograph.

respectively. Similarly, the austenitizing temperature did not significantly affect the tempered microstructures. The only variation in these cases is the austenitic grain size (Fig. 10). The fall in hardness, yield strength and tensile strength as well as ductility with increasing temperature of austenitizing is therefore attributed to the higher grain size.

In the case of lath martensite structures, the YS is related to the grain size by the empirical formula [9] :

$$\sigma_{ys} = \sigma_i + K c^{1/2} + K_y d^{-1/2} + \alpha \mathrm{Gbr}^{1/2}$$

where σ_{ys} is the yield strength of lath martensite, σ_i is the resistance to dislocation movement, c is the carbon content, K and K_y are Locking parameters, d is the packet size or grain size, G is the shear modulus, b is burgers vector and ρ is the dislocation density. These terms take care of the frictional force due to dislocation movement, solid solution strengthening, boundary resistance and strain hardening respectively. Though the grain size is not specifically mentioned here, the packet size (and not the lath size), which contains many laths, is directly related to individual grain size. Of the four factors in the above equation, the grain size and/or packet size is dependent strongly on austenitizing temperature. It is clear from the present investigation that a variation, as shown in Fig. 10, in grain size from $\sim$10 μm (at 925°C) to 250 μm (at 1250°C) resulted in a 10 to 15% decrease in

strength and hardness of the steel. The grain size value in the steel observed during the previous study [4] was close to 6 μm for the austenitizing temperature of 925°C. This variation could be due to the difference in the degree of deformation imparted to cast ESR ingots (grain size −25 μm) during thermo-mechanical processing.

However, the absence of any predominant recovery and recrystallization in the lath structure and the presence of fine cementite platelets explain the retention of high strength properties in the steel on tempering at 450°C.

Optical and transmission electron microscopy studies of the present investigation shows that the austenitizing temperature, apart from affecting the grain size (uniformly for all cooling rates) has influenced the basic microstructure significantly only in the furnace cooled condition. The microstructure changed from massive ferrite – fine pearlite at lower temperatures (∼925°C) to bainite at higher temperatures of austenitizing (Fig. 11). Equiaxed ferrite or coarse pearlite did not form due to the high alloy content of the steel. Similar results were also reported earlier by Viswanathan and Joshi [10]. In the case of air-cooling, mixed structures of upper bainite and lower bainite formed for all austenitizing temperatures (Fig. 12). This result supports the findings of Buchi et al. [11]. In the case of oil quenching also, lath martensite structures only were observed in all cases and the packet size of martensite, not the lath size, was affected by the austenitizing temperature. The precipitation of ε-carbide on tempering the present steel at 200°C (Fig. 14) was also reported by Suresh et al [4]. The structure corresponded to $Fe_{2.4}C$ with lattice parameters; $c = 4.33$ Å, $a = 2.73$ Å, $c/a = 1.58$ irrespective of the austenitizing temperature. The samples tempered at 450°C showed typical tempered martensite structure with profuse precipitation of cementite within the lath as well as on the lath boundaries. Tipler et al. [12] also reported similar tempered martensite in rotor steel after austenitizing at different temperatures (950°C, 1050°C and 1300°C) followed by oil quenching and tempering at 500°C for 1 hr. No retained austenite could be detected in the steel during the present investigation. The microstructural features are too fine to be resolved by optical microscopy and quantitative characterization by TEM is difficult. A qualitative assessment only has therefore been carried out now. However a detailed study on the effect of different tempering temperatures, ranging up to 600°C, on the microstructure and properties of this steel was carried out earlier and presented [4].

The sub-size Charpy impact energy has not significantly altered with austenitizing temperature when the steel was oil quenched and tempered at 200°C. Previous work by Horn and Ritchie [13] as well as by Thomas [14] showed that the impact energy of as-quenched steels in fact improves with increasing austenitizing temperature and they attributed to higher amounts of retained austenite with coarser grain sizes. Precipitation of fine ε–carbide due to 200°C tempering must have offset this increase to result in a nearly uniform value. However, the impact energy fell drastically as the austenitizing temperature increased for the 450°C tempered steel (Fig. 6) due to the precipitation of cementite both along the lath boundaries and within the laths. Further, coagulation of these precipitates takes place which increases their size leading to enhanced slip distance. This results in less hindrance to the initiation and propagation of cracks. The decrease in impact energy is more severe as compared to the fall in hardness or tensile properties [15, 16].

In summary it may be stated that while there has been a distinct difference in the grain size due to variation in the austenitizing temperature, this has not resulted in a change (except in furnace cooled condition) in the basic microstructure of the steel for a given cooling rate. The decrease in hardness, yield strength and ultimate tensile strength of the steel is therefore mainly attributable to the change in the austenitic grain size as the austenitizing temperature is increased. The present investigation helps in understanding the wide range of microstructures and mechanical properties that can be obtained in this steel in various regions of the heat affected zone of a weld.

5. Conclusions

The following conclusions may be drawn on the basis of the present investigations on the influence of austenitizing temperature on the structure and properties of 0.3C-CrMoV(ESR) steel.

1. The austenite grain size increases from about 10 μm to 250 μm as the austenitizing temperature is increased from 925°C to 1250°C (1 hr).
2. The YS, UTS and hardness of the steel decrease as the austenitizing temperature is increased from 925°C to 1250°C for 1 hr for all cooling rates (furnace cooling, air cooling, oil quenching, quenching and tempering at 200°C, quenching and tempering at 450°C). The ranges of microstructures that can be obtained in the heat-affected zone are massive ferrite, fine pearlite, upper as well as lower bainite and martensite.
3. The decrease in hardness, yield strength and ultimate tensile strength of the steel are mainly attributable to the change in the austenitic grain size as the austenitizing temperature is increased.
4. The sub-size Charpy impact energy for the oil quenched steel tempered at 200°C did not vary significantly with austenitizing temperature but decreased drastically when the steel was tempered at 450°C.

Acknowledgement

The authors thankfully acknowledge their gratitude to Dr. B N Suresh, Director, VSSC for granting permission to publish this paper in this journal.

References

1. French Norms for Steel Products (AFNOR-BNS), Spec. no. A35-55A, Paris, France **1** (1978) 299.

2. K. SREEKUMAR, M. S. P. MURTY, A. NATARAJAN and P. P. SINHA, *Trans. Indian Inst. Met.* **35** (1982) 349.
3. J. M. HOLT, H. MINDLIN and C. Y. HO, Structural Alloys Hand-Book CINDAS/Purdue University, West Lafayette, Indiana, USA, 1996 vol. 1.
4. M. R. SURESH, I. SAMAJDAR, A. INGLE, N. B. BALLAL, P. K. RAO and P. P. SINHA, *Iron. Steel.* **30** (2003) 379.
5. M. CHATTERJEE, M. S. N. BALASUBRAMANIAN, K. M. GUPT and P. K. RAO, *Ironmaking and Steelmaking* **17** (1990) 38.
6. G. M. PADKI, M. S. N. BALASUBRAMANIAN, K. M. GUPT and P. K. RAO, *ibid.* **10** (1983) 180.
7. G. HOYLE, Electroslag Processes: Principles and Practice (Applied Science Publishers, London & New York, 1983).
8. M. R. SURESH, Development of a New Ultrahigh Strength Steel and Studies of its Microstructure and Properties, Ph.D. Thesis, IIT, Bombay, 2002.
9. L. A. NORSTORM, *Scand. J. Metall.* **5** (1976) 159.
10. R. VISHWANATHAN and A. JOSHI, *Met. Trans. A.* **6A** (1975) 2289.
11. G. J. P. BUCHI, J. H. R. PAGE and M. P. SIDEY, *J. Iron. Steel. Inst.* **203** (1965) 291.
12. H. R. TIPLER, L. H. TAYLOR and G. B. THOMAS, *Metal. Tech.* **2** (1975) 206.
13. R. M. HORN and R. O. RITCHIE, *Met. Trans. A.* **9A** (1978) 1039.
14. G. THOMAS, *Met. Trans. A.* **9** (1978) 439.
15. G. R. SPEICH, D. S. DABKOWSKI and L. F. PORTER, *Met. Trans.* **4** (1973) 303.
16. P. M. MACMEIER, C. D. LITTLE. M. H. HOROWITZ and R. P. OATES, *Metal. Tech.* (1979) 291.

Received 25 May
and accepted 29 August 2005